

## Oxidation induced precipitation in Al implanted epitaxial silicon

A. La Ferla, G. Galvagno, P. K. Giri, G. Franzò, and E. Rimini

*Dipartimento di Fisica ed Astronomia dell'Università di Catania, INFN, Corso Italia 57, I-95129 Catania, Italy*

V. Raineri

*CNR-IMETEM, Stradale Primosole 50, I-95121 Catania, Italy*

A. Gasparotto

*Dipartimento di Fisica dell'Università di Padova, Via Marzola 8, I-35131 Padova, Italy*

D. Cali

*STMicroelectronics, Stradale Primosole 50, I-95121 Catania, Italy*

(Received 11 February 2000; accepted for publication 13 July 2000)

The behavior of Al implanted in silicon has been investigated during thermal oxidation. It has been found that precipitation of Al into Al–O-defect complexes depends on the implant energy, i.e., on the distance of the dopant from the surface. It occurs at 650 keV, but it does not at 2.0 MeV or higher energies. This phenomenon has been explained taking into account the diffusivity of self-interstitials introduced during oxidation, the oxygen present in the Si, the Al concentration, and the annealing out of defects. © 2000 American Institute of Physics. [S0021-8979(00)06120-X]

### INTRODUCTION

Al is the fast diffusing *p*-type dopant in Si and is a good candidate for the fabrication of deep *p* wells in power devices. The main problems associated with the use of Al implants, however, are the outdiffusion from the sample during the driving process<sup>1</sup> and its reactivity with oxygen atoms.<sup>2,3</sup> The latter phenomenon causes Al precipitation in proximity to the implant-induced defects that act as nucleation centers for the formation of Al<sub>x</sub>O<sub>y</sub> clusters. This occurs in Czochralski-grown substrates where the bulk oxygen concentration is about  $8 \times 10^{17}$  atom/cm<sup>3</sup>. Indeed, the precipitation is absent in epitaxial layers where the oxygen content is less than  $1 \times 10^{16}$  atom/cm<sup>3</sup>, or if the presence of defects is avoided as, for instance, by Al predeposition.<sup>2,4</sup> Otherwise, even for Al implants in epitaxial layers, precipitation might occur if thermal oxidation processes are employed for the device fabrication.<sup>5</sup> In fact, during oxidation, oxygen is introduced at a concentration about one order of magnitude higher than the equilibrium solid solubility characteristic of samples well annealed in an inert ambient. The enhanced oxygen solubility has been associated with a metastable equilibrium of the dissolved oxygen with the oxidizing ambient and characterized by an excess of the chemical potential.<sup>7</sup> This phenomenon is also responsible for the growth in thickness of buried oxides in Si-on-insulator structures where the superficial Si layer is thermally oxidized.<sup>11</sup>

In this work, we have investigated the influence of the Al<sup>+</sup> ion energy on the precipitation, after thermal oxidation processes, for implants into epitaxial silicon samples.

### EXPERIMENT

Aluminum ions were implanted into epitaxially grown *n*-type silicon wafers at 650 keV, 6 MeV, and 9.3 MeV energies and a dose of  $4 \times 10^{14}$  atom/cm<sup>2</sup>. The implants were

performed at room temperature using a 1.7 MV TANDETRON implanter. The samples were then thermally processed in a horizontal furnace at 1200 °C in N<sub>2</sub> or O<sub>2</sub> ambient for different times. Before analysis, the oxide grown during the thermal process was etched off. The Al and O distributions were obtained by secondary ion mass spectrometry (SIMS) measurements performed with a CAMECA IMS 4f machine. A 5.5 keV O<sub>2</sub><sup>+</sup> primary beam was used to profile the Al species and a 14.5 keV Cs<sup>+</sup> primary beam for the oxygen distributions. Transmission electron microscopy (TEM) was performed using a JEOL 2010 FX microscope operating at 200 kV accelerating voltage. Samples were prepared in cross section using the standard procedure.

### RESULTS AND DISCUSSION

When aluminum is implanted even below its solid solubility in silicon substrates, precipitation takes place if oxygen is present in the damped region. To avoid this phenomenon the implants were performed in epitaxial layers, with an oxygen content lower than  $1 \times 10^{16}$  atom/cm<sup>3</sup>. The SIMS analyses of the aluminum distributions for the 650 keV and 6 MeV  $4 \times 10^{14}$  atom/cm<sup>2</sup> implants are shown in Figs. 1(a) and 1(b), respectively. The samples were annealed in N<sub>2</sub> ambient at 1200 °C for 1 h. The profiles follow the normal diffusion distribution: all the implanted Al atoms are free to diffuse and electrically active. The impurity atoms that reach the surface during the thermal diffusion escape from the sample and for this reason a depletion of Al in the surface region is observed. The profiles can be simulated solving the diffusion equation of Al in Si and taking into account the escape from the surface.<sup>6</sup>

If the thermal process is performed in O<sub>2</sub> ambient, Al can precipitate due to its interaction with the injected oxygen.<sup>5</sup> The SIMS analyses of Figs. 2(a) and 2(b) report the Al and O profiles, respectively, in the 650 keV

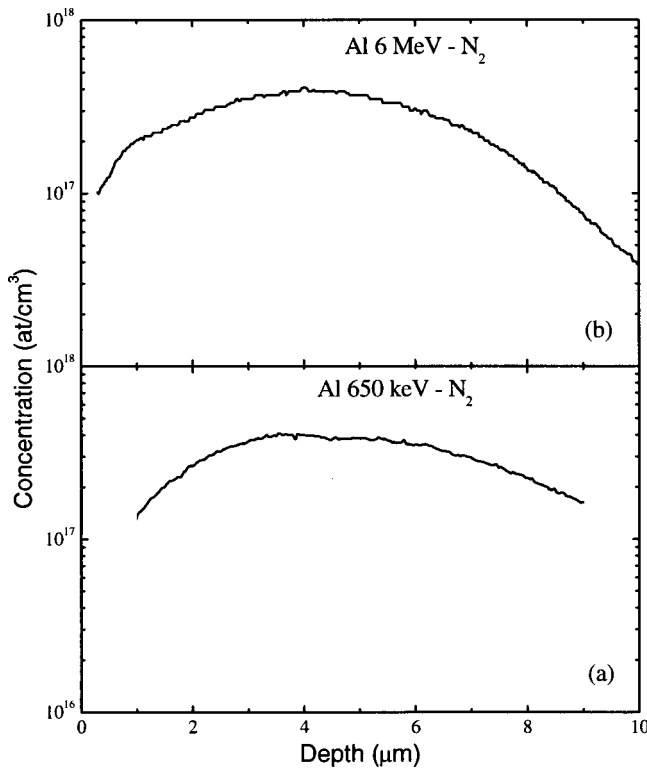


FIG. 1. SIMS profiles of:  $4 \times 10^{14}/\text{cm}^2$  650 keV (a) and  $4 \times 10^{14}/\text{cm}^2$  6 MeV (b) Al implanted sample, after diffusion at 1200 °C for 1 h in N<sub>2</sub> ambient.

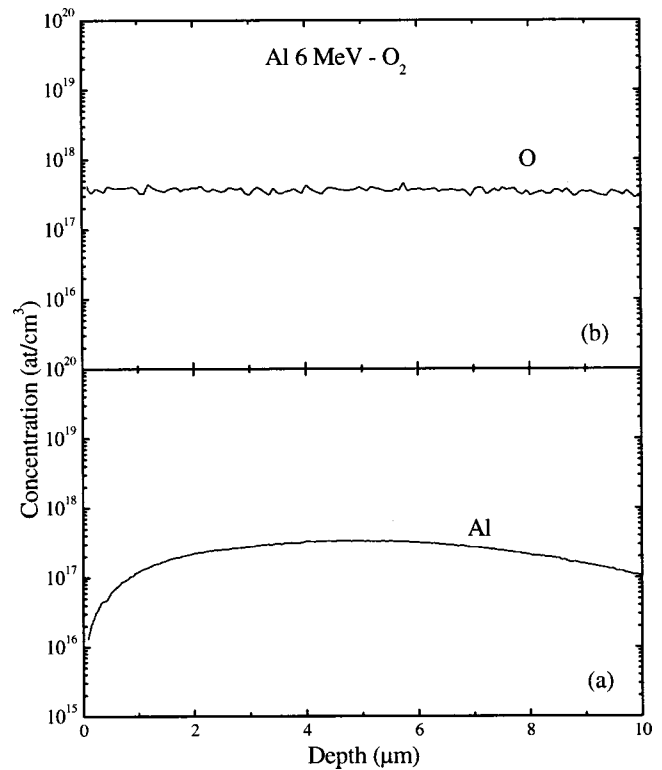


FIG. 3. Al (a) and O (b) SIMS depth profile of a sample implanted with  $4 \times 10^{14}/\text{cm}^2$  Al at 6 MeV after a dry oxidation at 1200 °C for 1 h.

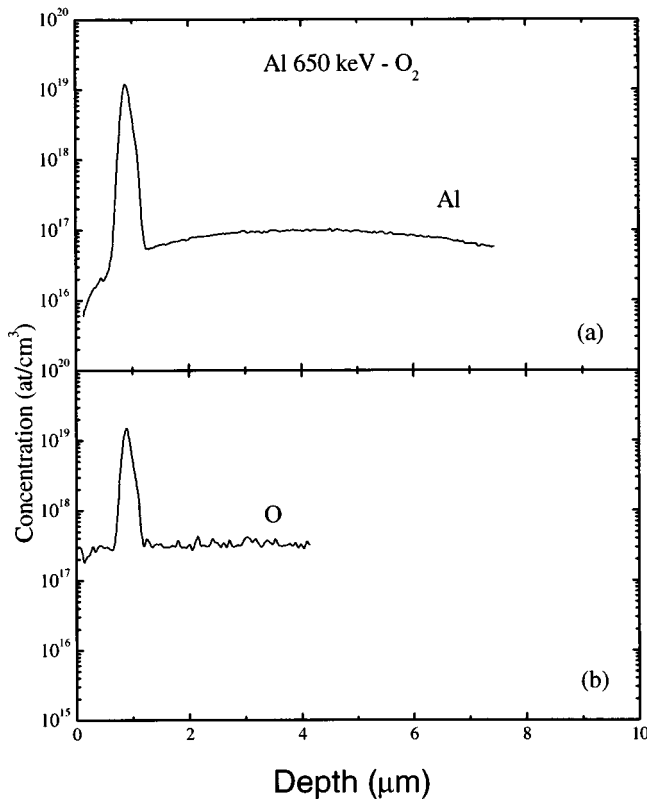


FIG. 2. Al (a) and O (b) SIMS profiles of  $4 \times 10^{14}/\text{cm}^2$  650 keV Al implanted sample, after a dry oxidation at 1200 °C for 1 h.

$4 \times 10^{14}$  atom/cm<sup>3</sup> implanted wafer. This sample was processed in O<sub>2</sub> ambient at a temperature of 1200 °C for 1 h. During oxidation not all the oxygen atoms react with Si at the Si/SiO<sub>2</sub> interface, a fraction of them penetrates into the Si substrates as free atoms. It was demonstrated<sup>7</sup> that during steam oxidation oxygen penetrates into Si at a concentration higher than its solid solubility. Because the diffusion coefficient of interstitial oxygen is about one order of magnitude higher than that of Al (at 1200 °C  $D_{\text{O}} = 3 \times 10^{-10}$  cm<sup>2</sup>/s and  $D_{\text{Al}} = 10^{-11}$  cm<sup>2</sup>/s), these two species can interact before a substantial redistribution of Al takes place. Precipitation occurs immediately at the damage peak depth. In fact, the profiles clearly show Al and O precipitation at a depth of about 1 μm, i.e., the Al 650 keV projected range.

Increasing the beam energy from 650 keV to 6 MeV, a quite different distribution for Al and O is obtained, as shown by the corresponding SIMS profiles reported in Figs. 3(a) and 3(b). The Si sample was implanted with 6 MeV Al<sup>+</sup> to a dose of  $4 \times 10^{14}$  atom/cm<sup>3</sup> and processed at 1200 °C for 1 h in O<sub>2</sub> ambient. In spite of the same adopted thermal process, precipitation does not occur in this sample. The Al distribution follows the usual diffusion behavior in Si at 1200 °C, and the O concentration is everywhere lower than the detection limit of the SIMS analysis. A prolonged thermal oxidation indicates that precipitation occurs only for the lower energy. Similar results have been obtained at energies higher than 6 MeV.<sup>10</sup>

The TEM cross-sectional analysis (Fig. 4) of the 650 keV implanted sample shows the presence of dislocations (of about 1 μm in length between the Si/SiO<sub>2</sub> interface and the end of range) and of agglomerates (less than 10 nm in diam-

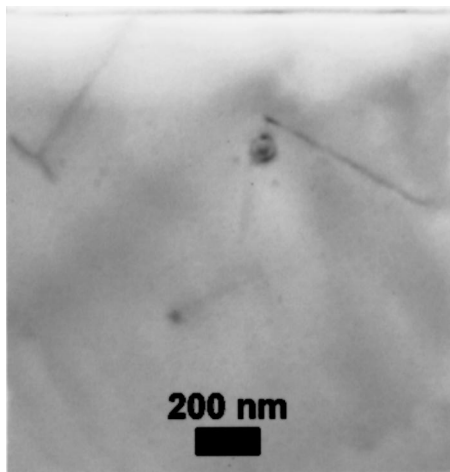


FIG. 4. Cross-sectional TEM analysis of 650 keV  $4 \times 10^{14}/\text{cm}^2$  Al implanted sample and dry oxidized at 1200 °C for 4 h.

eter). Defects and precipitates are not detected in the samples implanted at higher Al energies. It has been demonstrated in previous works that precipitation occurs where damage, aluminum, and oxygen are simultaneously present.<sup>2-4</sup>

To understand the phenomenon taking place during oxidation, the injected oxygen distribution has been calculated using the model described in Ref. 11. It assumes the increase of the interstitial oxygen concentration at the  $\text{SiO}_2/\text{Si}$  interface  $\Delta C_i^O$  is assumed to be proportional to the oxidation rate

$$\Delta C_i^O(t, T) = \beta(T) \cdot v_{\text{ox}}(t), \quad (1)$$

where  $\beta(T)$  is a temperature dependent parameter that can be determined from experimental results for dry and wet oxidation,<sup>3,4</sup> while  $v_{\text{ox}}(t)$  is the oxide growth velocity. From Eq. (1) it is clear that when the oxidation rate decreases, from the linear to the parabolic regime, the amount of the injected oxygen is also reduced, and oxygen must now diffuse through a thicker oxide layer.

Figure 5 reports the calculated oxygen profiles after 1 min of dry oxidation at 1000, 1100, 1200, and 1300 °C, respectively. These distributions were obtained by solving nu-

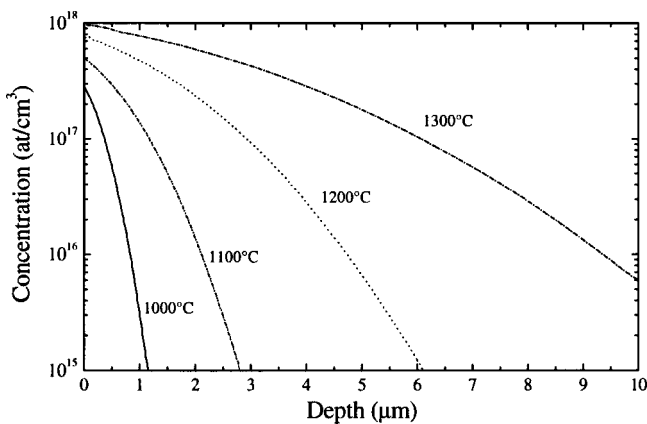


FIG. 5. Calculated oxygen redistribution in the Si substrate after dry oxidation performed for 1 min at different temperatures.

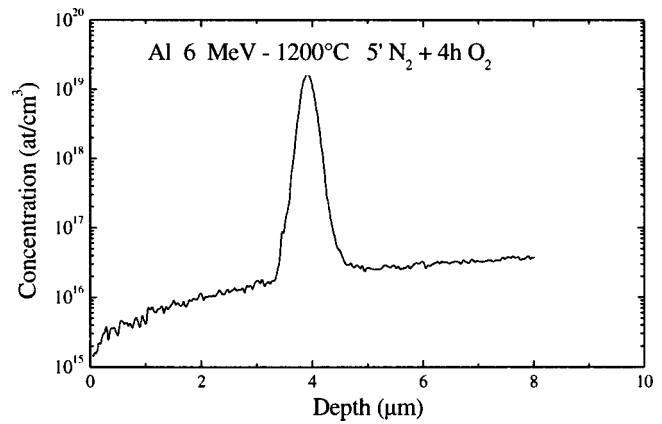


FIG. 6. Al profile of 6 MeV  $4 \times 10^{14}/\text{cm}^2$  Al implanted sample after a thermal process at 1200 °C in  $\text{N}_2$  ambient for 5 min and dry oxidized at the same temperature for 4 h.

merically the diffusion equation for oxygen transport in silicon with the following boundary condition (for  $x=0$ ) at the  $\text{SiO}_2/\text{Si}$  interface:

$$C_i^O(t, T) = C_{\text{ieq}}^O(T) + \Delta C_i^O(t, T). \quad (2)$$

Here  $C_{\text{ieq}}^O(T)$  is the equilibrium solid solubility of interstitial oxygen in silicon and  $\Delta C_i^O(t, T)$  is obtained from Eq. (1). This boundary condition changes with time because the oxygen introduction decreases with the oxide thickness.

Precipitation of Al occurs when the oxygen concentration around the damaged region exceeds  $10^{17}$  atom/ $\text{cm}^3$ . The data of Fig. 5 indicate that just slightly more than 1 min at 1200 °C is enough to reach this threshold value at a distance from the surface deeper than 4  $\mu\text{m}$ , i.e., the projected range of the 6 MeV Al implant. Probably at such high temperature, although for a short time, the damage might anneal out before the oxygen arrival, thus Al precipitation could be avoided. At lower depth corresponding to lower energies, like 650 keV, high O concentrations are reached after just a few seconds. During such a short time the damage does not anneal out completely and precipitation occurs. To test this hypothesis the sample implanted with 6 MeV  $4 \times 10^{14}$  Al/ $\text{cm}^2$  was annealed at 1200 °C in  $\text{N}_2$  ambient for 5 min and then dry oxidized at 1200 °C for 4 h. The SIMS Al profile is reported in Fig. 6. A peak of precipitated Al is clearly present at a depth of 4  $\mu\text{m}$ . Also the TEM image reported in Fig. 7(a) shows a band of dislocation loops and of precipitates both located at the same depth. This means that the high temperature process for few minutes in  $\text{N}_2$  ambient is unable to anneal the implant damage. This result does not agree with the previous considerations on the simple relationship between annealing time, oxygen diffusion length, and depth of the implant.

Other factors should then play a role in the experiments performed under oxidation, and a more detailed analysis of the interaction between defects and impurities is required. Our results, for instance, can be justified if the interaction of Al with vacancies is stronger than with interstitials. This implies that during the first stage of any thermal processes self-interstitials leave the damaged region and an excess of vacancies ( $V$ ) remains, giving rise to Al- $V$  complexes. During

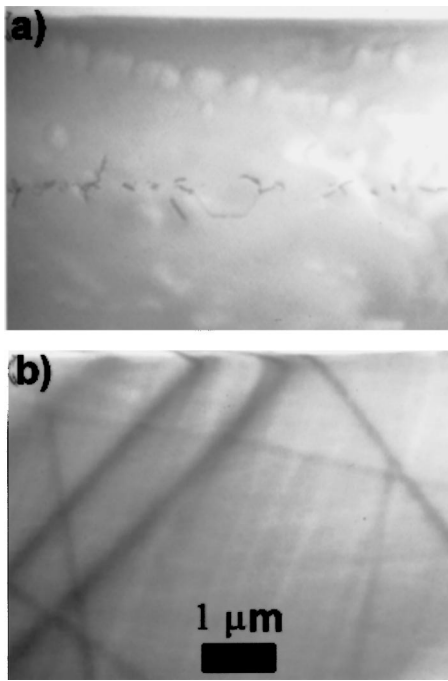


FIG. 7. Cross-sectional TEM analysis of 6 MeV,  $4 \times 10^{14}/\text{cm}^2$  Al implanted sample dry oxidized at 1200 °C for 4 h, with a preannealing at 1200 °C for 5 min in  $\text{N}_2$  ambient (a); without preannealing (b).

oxidation the sample is traversed not only by a flux of oxygen but also by self-interstitials rather than form stacking faults. The two species are characterized by a different diffusion coefficient,  $10^{-10} \text{ cm}^2 \text{ s}^{-1}$  (at 1200 °C) for O and  $10^{-5} \text{ cm}^2 \text{ s}^{-1}$  for interstitials. Complex Al-V can be eliminated by the highly mobile self-interstitials before the arrival of oxygen, thus preventing the formation of more stable defects, and then of precipitates.

The TEM image of Fig. 7(b) supports this mechanism. The sample implanted with 6 MeV  $4 \times 10^{14} \text{ Al}/\text{cm}^2$  and oxidized at 1200 °C for 4 h is free of dislocations and of a precipitate band, defects that are instead present in the preannealed sample. To estimate the concentration of interstitials able to anneal the damage (Al-V complexes) a model developed by Hu<sup>8</sup> has been adopted. This model is based on two assumptions: (1) thermal oxidation injects self-interstitials at a rate that is directly proportional to the rate of thermal oxidation; (2) the excess self-interstitials flood the bulk and at the same time annihilate at the Si/SiO<sub>2</sub> interface via a surface regrowth process. The rate of annihilation at the interface is directly proportional to the concentration of excess interstitials and to the concentration of surface sinks, considered to be ledge kinks.

To determine the depth distribution of self-interstitials in the Si bulk, it is necessary to solve the following continuity equation:

$$\frac{\partial C_I}{\partial t} = D_I \frac{\partial^2 C_I}{\partial x^2} \quad (3)$$

with the boundary condition at the Si/SiO<sub>2</sub> interface

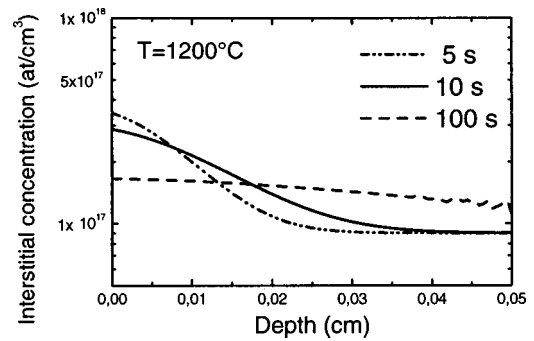


FIG. 8. Computed self-interstitial distributions for oxidation at 1200 °C for 1, 5, and 10 s.

$$-D_I \frac{\partial C_I}{\partial x} = R_g - R_r, \quad (4)$$

where  $D_I$  is the diffusion coefficient of interstitials and  $C_I$  is the concentration of self-interstitials.

Then, the production of excess self-interstitials is due to equilibrium between the generation and the recombination rate at the Si/SiO<sub>2</sub> interface. The generation rate ( $R_g$ ) can be written as:  $R_g = A \times t^{1/2}$  (parabolic regime), while the surface annihilation rate ( $R_r$ ) can be expressed as:  $R_r = K \times (C_I - C_I^*)$ , where  $C_I^*$  represents the interstitial equilibrium concentration.  $A$  and  $K$  are two parameters.

From the derivation of the continuity Eq. (1), Hu determines an analytical expression for the self-interstitials depth distribution.<sup>9</sup> To perform a quantitative analysis of the interstitial concentration profile, the parameters  $A$  and  $K$  must be estimated. On key and the physical meaning of these parameters, if the rate of generation is a function of the silicon oxidized atoms, then the parameter  $A$  depends on this fraction and on the parabolic rate constant. The physical meaning of the parameter  $K$  is the self-interstitial annihilation rate at the interface and  $D_I/K^2$  is the lifetime of the interstitial excess.

Much experimental data are present in the literature about stacking fault growth during thermal oxidation processes<sup>13,14</sup> and the kinetics of this growth is related to the self-interstitial supersaturation. Hu expresses the stacking fault length as a function of the time with the formula

$$r(t) = 2 \times \pi \times a_0^2 \times D_I \times \frac{A}{K} \times t^{1/2}, \quad (5)$$

where  $a_0$  is the radius of the annihilation centers and  $A$  and  $K$  are the same parameters as above. Then, fitting the experimental literature data on the stacking fault length with Eq. (5), for dry oxidation of  $\langle 100 \rangle$  Si at a temperature of 1200 °C, using for  $a_0 = 3.85 \times 10^{-8} \text{ cm}$  and  $D_I = 10^{-5} \text{ cm}^2/\text{s}$ , we obtain a value for the ratio  $A/K = 1 \times 10^{17} \text{ s}^{1/2} \times \text{cm}^{-3}$ . With this value it is possible to calculate the self-interstitial depth distributions and they are shown in Fig. 8 for 5, 10, and 100 s of oxidation. From a comparison between Figs. 5 and 8 we deduce that 10 s are enough for self-interstitials to reach a value of about  $3 \times 10^{17} \text{ atom}/\text{cm}^3$  in correspondence to the ion implantation damaged region, while oxygen needs more time. For this

reason at the higher adopted implant energies, the oxygen arrival delay allows the self-interstitials to remove the implantation damage. Indeed, for a depth of 1  $\mu\text{m}$  (corresponding to the projected range of the 650 keV implant), the oxygen arrival does not permit the damage annihilation by self-interstitials, as this depth is very close to the interface. A simpler estimate of the time needed to anneal out the Al–V complexes before the arrival of oxygen is presented in the following. During oxidation the generation rate of excess Si interstitial per unit area at the Si/SiO<sub>2</sub> interface is proportional to the velocity of interface movement  $v$  as given by<sup>12</sup>

$$G = \frac{\gamma v}{\Omega} = \frac{\gamma a}{\Omega} \left( \frac{dx}{dt} \right), \quad (6)$$

where  $\gamma$  indicates the fraction of excess silicon at the interface and it ranges between 0 and 0.55,  $a$  is the well-known ratio 0.44 between the oxidation rate and the interface velocity, and  $\Omega$  is the volume of a silicon atom. At an oxidation rate of  $\approx 1 \mu\text{m/h}$  typical of a dry oxidation at 1200 °C, the excess silicon atoms are generated at a rate of  $1.3 \times 10^{18}$  atoms/(h $\times$ cm<sup>2</sup>) from the previous relation with  $\gamma=0.55$ . The largest part of these interstitials recombines in the oxide with the arriving O<sub>2</sub> molecules; it has been estimated<sup>12</sup> by analysis of oxidation stacking faults that only  $3 \times 10^{-3}$  of all the interstitials is injected into bulk silicon, i.e., a flux of  $4 \times 10^{15}$  atom/(h $\times$ cm<sup>2</sup>) is available for recombination with vacancies of the Al–V complexes. As a simple guess one might assume that to anneal out the Al–V defects one needs an integrated flux of self-interstitials on the order of the implanted dose, i.e.,  $F_I \times t \geq 4 \times 10^{14}/\text{cm}^2$ ; this implies a time of about 360 s. According to the diffusivity of O at 1200 °C  $\approx 10^{-10}$  cm<sup>2</sup>/s, the depth of 1  $\mu\text{m}$  is reached after 10<sup>2</sup> s while that of 4  $\mu\text{m}$  is reached after  $1.6 \times 10^3$  s. The previous estimate indicates that for the 650 keV Al implant the integrated flux of interstitials is not enough to anneal the vacancies before the arrival of oxygen, thus causing a precipitation of Al–O–V etc.

## CONCLUSIONS

In this work the Al precipitation induced by thermal oxidation has been investigated. In particular precipitation de-

pends on the implantation energy: it occurs for the 650 keV Al implant, while it does not for the higher investigated one (6 MeV). This effect has been explained taking into account the injection of oxygen and Si self-interstitial atoms during oxidation and their interaction with Al atoms and damage induced by ion implantation. In fact, it has already been demonstrated that when Al atoms interact with oxygen and defects, precipitation occurs. But for the higher investigated Al implantation energy, the Si self-interstitials that reach the damaged region before the oxygen atoms, are able to remove the implantation defects, mainly in the form of Al–V complexes, thus avoiding precipitation. In the case of lower energy (650 keV) the proximity between the Al profile and the surface does not allow the damage to be completely annihilated before the oxygen arrives in the last case, when Al precipitation occurs.

<sup>1</sup>G. Galvagno, F. La Via, F. Priolo, and E. Rimini, *Semicond. Sci. Technol.* **8**, 488 (1993).

<sup>2</sup>G. Galvagno, A. La Ferla, C. Spinella, F. Priolo, V. Raineri, L. Torrisi, E. Rimini, A. Carnera, and A. Gasparotto, *J. Appl. Phys.* **76**, 2070 (1994).

<sup>3</sup>A. La Ferla, L. Torrisi, G. Galvagno, E. Rimini, G. Ciavola, A. Carnera, and A. Gasparotto, *Appl. Phys. Lett.* **62**, 393 (1993).

<sup>4</sup>A. La Ferla, L. Torrisi, G. Galvagno, E. Rimini, G. Ciavola, A. Carnera, and A. Gasparotto, *Nucl. Instrum. Methods Phys. Res. B* **74**, 109 (1993).

<sup>5</sup>E. Rimini, G. Galvagno, A. La Ferla, V. Raineri, G. Franco, M. Camalleri, A. Gasparotto, and A. Carnera, *Proceedings IIT'96*, 654 (1997).

<sup>6</sup>B. E. Deal and A. S. Grove, *J. Appl. Phys.* **36**, 3770 (1965).

<sup>7</sup>J. C. Mikkelsen, Jr., *Appl. Phys. Lett.* **41**, 871 (1982).

<sup>8</sup>S. M. Hu, *Mater. Sci. Eng., R.* **13**, 105 (1994).

<sup>9</sup>S. M. Hu, *Atomic Diffusion in Semiconductors*, edited by D. Shaw (Plenum, New York, 1973), in Chap. V; S. M. Hu, *Appl. Phys. Lett.* **43**, 449 (1983).

<sup>10</sup>A. Seeger and K. P. Chik, *Phys. Status Solidi* **29**, 455 (1968).

<sup>11</sup>U. Gösele, E. Schroer, and J. Y. Huh, *Appl. Phys. Lett.* **67**, 241 (1995).

<sup>12</sup>A. Lin, R. W. Dutton, D. A. Antoniadis, and W. A. Tiller, *J. Electrochem. Soc.* **128**, 1121 (1981).

<sup>13</sup>S. P. Murarka and G. Quintana, *J. Appl. Phys.* **48**, 46 (1977).

<sup>14</sup>S. M. Hu, *Appl. Phys. Lett.* **27**, 165 (1975).